

## Electron synchrotron radiation in the far infrared

Duncan J. Wingham\*

*Department of Physics and Astronomy, Mullard Space Science Laboratory, University College London, Holmbury Saint Mary, Dorking, Surrey, RH5 6NT England*

(Received 23 May 1986)

Recent installations at a number of synchrotron light facilities have extended the use of the synchrotron radiation spectrum into the far infrared. At these low frequencies, it is not self-evident that the high-frequency, far-field expressions used normally to describe the synchrotron spectrum are valid. In this paper this question is examined. The near-field distance of the synchrotron source, analogous to the Rayleigh distance of conventional sources, is derived. It is shown that at wavelengths from cm to mm<sup>-1</sup> this distance is of the order of 1 m, which is sufficient to influence the siting of an initial aperture. The effect of the finite length of the curved sections of the electron orbit is investigated and it is shown that structure on the  $\pm 10$ -dB level is introduced into the spectrum at these wavelengths. Finally, the temporal and spatial coherence of the field is examined. It is demonstrated that no coherent radiation is to be expected from the synchrotron at these wavelengths, but that at mm wavelengths the field will be spatially coherent over apertures of order 100 mrad.

### I. INTRODUCTION

A number of synchrotron light facilities have recently been equipped with ports whose purpose is to extend the use of synchrotron radiation into the far-infrared region of the synchrotron spectrum.<sup>1</sup> The use of the electron synchrotron in the infrared has been discussed by a number of authors.<sup>2-4</sup> The advantages of high brightness and high flux offered by the synchrotron over broadband laboratory sources has been discussed by Duncan and Williams,<sup>5</sup> who also present estimates of the flux and brightness particular to the Daresbury and Brookhaven institutions.

These descriptions of the infrared properties of synchrotron radiation are based on the derivation, due to Schwinger,<sup>6</sup> of the high-frequency field radiated by a relativistic electron in circular motion. In the far-infrared region of the synchrotron spectrum the wavelengths are sufficiently long that it is neither clear that the frequencies may be assumed to be high, nor that the departure of the electrons from a truly circular orbit may be ignored. In addition, when the radiated wavelength approaches that of the electron bunch length, coherent radiation from the electrons may become important, effecting both the spectral and spatial coherence of the radiated field. It is the purpose of this paper to establish the degree to which the high-frequency approximation may be used in the cm to mm<sup>-1</sup> region of the synchrotron spectrum, and describe the consequences of coherent radiation on the statistical properties of the field.

In Schwinger's derivation<sup>6</sup> of the synchrotron spectrum it is assumed *a priori* that the point at which the field is calculated is infinitely distant from the circulating electron. In an experimental system the collecting aperture is only finitely distant, and may be certainly much closer than the electron orbit radius. Yet, at high frequencies, the effect of the relativistic motion of the electron is to re-

strict that part of its orbit contributing to the radiated field at a particular point to those sections very close to the tangent ray from the orbit. At optical frequencies and above this behavior is certainly sufficient to regard the collecting aperture as being infinitely distant.

The length of orbit contributing to a given point varies as  $\omega^{-1/3}$ , and as the radiated frequency decreases, it becomes increasingly less obvious that this length may be regarded as small; that is, it becomes less obvious that the aperture lies in the far field of the synchrotron source. In Sec. II we derive the near-field distance of the synchrotron source and consider whether it is sufficiently large to influence the siting of an initial aperture.

In many synchrotrons the electrons do not, in fact, execute circular orbits.<sup>7</sup> The orbit consists of a number of circular arcs joined by linear sections of track. In the far infrared the length of orbit contributing to the field at a point may approach the length of the curved sections of track, and lead in turn to a lower radiated power than might otherwise be expected. In Sec. III we discuss the effect on the radiated field of the finite length of curved electron orbit.

The radiated field from the electron synchrotron is the summed effect of the field from successive bunches of  $10^{10}$  electrons. At high frequencies the electron bunch length is very large in comparison with the radiated wavelength, and the electrons may be considered as radiating completely incoherently. When the radiated frequency approaches the bunch length, however, this is no longer true. The cm to mm<sup>-1</sup> region of the radiated spectrum is particularly interesting because it is at these frequencies that coherent radiation may become dominant.<sup>8</sup> The radiation of coherent energy was a cause of some concern in the original design of synchrotrons,<sup>9</sup> but from the point of view of spectroscopy it is a desirable characteristic. Some evidence for coherent radiation in the far infrared is described in Ref. 5.

In Sec. IV we consider the statistical properties of the radiated field in the presence of coherent radiation. The spatial coherence of synchrotron radiation is the subject of papers by Benard and Rousseau,<sup>10</sup> and Akhmanov *et al.*<sup>11</sup> These papers leave the subject in a somewhat unsatisfactory state, inasmuch as the latter claim explicitly to contradict the former. We demonstrate that their results are, in fact, in agreement. The presence of a coherent component within the field, however, allows for radiation from different bunches to interfere with each other. This is of particular importance in the far infrared, where resolving powers of  $\sim$  MHz are possible. It is therefore desirable to include the effect of multiple bunches within a coherence calculation, and in Sec. IV we extend these calculations to include multiple bunches.

Finally, in Sec. V we bring these theoretical results together by considering their implications in the far-infrared region of the synchrotron spectrum, taking the post high brightness lattice (HBL) Daresbury synchrotron as an example.

## II. NEAR-FIELD EFFECTS FROM A SINGLE RADIATING ELECTRON

The spatial and spectral variation in the far-field, high-frequency field radiated to a point  $P$  from a relativistic electron in a circular orbit may be parametrized by three variables: the length  $\kappa$  of the tangent ray to  $P$  from the orbit, the angle  $\psi$  that the tangent ray makes with the plane of the electron orbit, and the ratio  $\nu$  of the radiated to orbital frequencies. In this section we address three questions. What is the length  $\kappa_0$  which  $\kappa$  must exceed before the point  $P$  may be assumed to be in the far field? For what range of angles  $\psi$  may the usual far-field result hold? Over what range of  $\nu$  can the frequencies be assumed high?

We consider the radiated field from an electron executing one cycle of the circular orbit shown in Fig. 1, without restricting the field point  $P$  to be infinitely distant. The field  $\mathbf{E}(\mathbf{x}, t)$  is given by

$$\mathbf{E}(\mathbf{x}, t) = -(1/c) \frac{\partial \mathbf{A}(\mathbf{x}, t)}{\partial t} - \nabla \phi(\mathbf{x}, t), \quad (2.1)$$

where the retarded vector and scalar potentials are

$$\mathbf{A}(\mathbf{x}, t) = \int \int \frac{\delta(t-t' - |\mathbf{x}-\mathbf{x}'|/c)}{|\mathbf{x}-\mathbf{x}'|} \times [\mathbf{J}(\mathbf{x}', t')/c] d\mathbf{x}' dt' \quad (2.2)$$

and

$$\mathbf{A}(\mathbf{x}, t) = \frac{e/c}{(2\pi)^{1/2}} \int_0^T \frac{\dot{\mathbf{R}}(t')}{|\mathbf{x}-\mathbf{R}(t')|} \exp\{-i[\omega t + k|\mathbf{x}-\mathbf{R}(t')|]\} dt' \quad (2.9)$$

and

$$\phi(\mathbf{x}, t) = \frac{e}{(2\pi)^{1/2}} \int_0^T \frac{1}{|\mathbf{x}-\mathbf{R}(t')|} \exp\{-i[\omega t + k|\mathbf{x}-\mathbf{R}(t')|]\} dt' \quad (2.10)$$

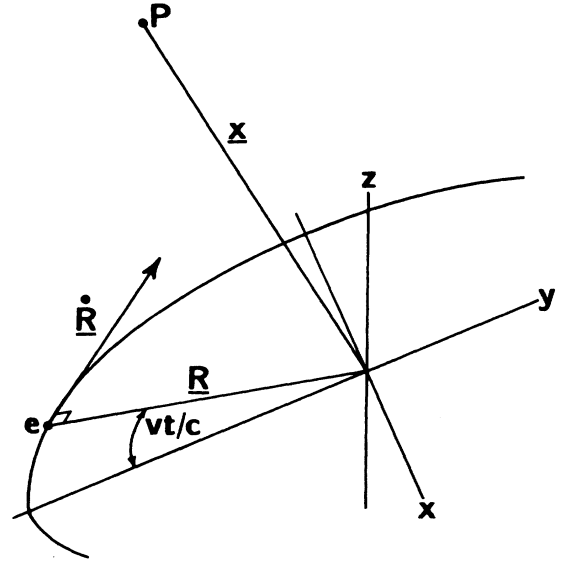


FIG. 1. The geometry of the synchrotron. The electron  $e$  traveling at a velocity  $v$  executes a circular orbit in the  $x$ - $y$  plane. Its position at any time  $t$  is given by the vector  $\mathbf{R}$ , which coincides with the positive  $y$  axis at  $t=0$ .

$$\phi(\mathbf{x}, t) = \int \int \frac{\delta(t-t' - |\mathbf{x}-\mathbf{x}'|/c)}{|\mathbf{x}-\mathbf{x}'|} \times \rho(\mathbf{x}', t) d\mathbf{x}' dt' \quad (2.3)$$

and the current and charge densities are given by

$$\mathbf{J}(\mathbf{x}, t) = e\delta(\mathbf{x}-\mathbf{R}(t))\dot{\mathbf{R}}(t), \quad (2.4)$$

$$\rho(\mathbf{x}, t) = e\delta(\mathbf{x}-\mathbf{R}(t)), \quad (2.5)$$

$$\mathbf{R}(t) = R \sin(vt/c)\mathbf{i} + R \cos(vt/c)\mathbf{j}, \quad (2.6)$$

and

$$0 \leq t \leq 2\pi R/v. \quad (2.7)$$

At the frequencies of interest  $\nu/c$  may be regarded as negligibly different from 1 and we set accordingly  $\nu$  equal to  $c$ .

The Fourier transform  $F(\omega)$  of a quantity  $f(t)$  is defined to be

$$F(\omega) = \frac{1}{(2\pi)^{1/2}} \int_{-\infty}^{\infty} f(t) \exp(i\omega t) dt \quad (2.8)$$

and from Eqs. (2.2)–(2.8) we find the Fourier-transformed potentials to be

which from Eqs. (2.1) and (2.3) are related to the Fourier-transformed field  $\mathbf{E}(\mathbf{x}, \omega)$  via

$$\mathbf{E}(\mathbf{x}, \omega) = -i\omega \mathbf{A}(\mathbf{x}, \omega) - \nabla \phi(\mathbf{x}, \omega). \quad (2.11)$$

At this point we remark that the far-field result may be derived by expanding the phase of the exponent and retaining only powers in  $t$  and  $t^3$ . (See, for example, Jackson.<sup>12</sup>) By analogy with more conventional sources, we might hope to shed some light on the near-field problem by including the ‘‘Fresnel’’ term in  $t^2$ . However, this leads immediately to an integral which is difficult to handle analytically. We therefore proceed in a rather less direct fashion, and seek a general integral form for the radiated field, and enquire under what circumstances it reduces to the far-field result.

With the identity

$$\frac{\exp(-ik|\mathbf{x}-\mathbf{R}|)}{|\mathbf{x}-\mathbf{R}|} = \frac{ik}{2\pi} \int_{-\pi/2}^{0-i\infty} \cos\psi d\psi \int_0^{2\pi} d\epsilon \exp[-ik\mathbf{n}\cdot(\mathbf{x}-\mathbf{R})], \quad (2.12)$$

where

$$\mathbf{n} = (\mathbf{i} \sin\epsilon + \mathbf{j} \cos\epsilon)\cos\psi + \mathbf{k} \sin\psi \quad (2.13)$$

and the positive limit is taken for  $z < 0$  and vice versa, the potentials may be written

$$\begin{aligned} \mathbf{A}(\mathbf{x}, \omega) = & \frac{iek}{c(2\pi)^{3/2}} \int d\psi \int d\epsilon \exp[-ikr \cos(\epsilon - \alpha)] \cos\psi \\ & \times \exp(-ikz \sin\psi) \int_0^T dt' \dot{\mathbf{R}}(t') \exp\{-i[\omega t' - kr \cos(ct'/R - \epsilon)]\}, \end{aligned} \quad (2.14)$$

$$\begin{aligned} \phi(\mathbf{x}, \omega) = & \frac{iek}{(2\pi)^{3/2}} \int d\psi \int d\epsilon \exp[-ikr \cos(\epsilon - \alpha)] \cos\psi \\ & \times \exp(-ikz \sin\psi) \int_0^T dt' \exp\{-i[\omega t' - kr \cos(ct'/R - \epsilon)]\}. \end{aligned} \quad (2.15)$$

Performing the integrations over  $t'$  in Eqs. (2.14) and (2.15), substituting the result in Eq. (2.11), and collecting terms according to their component results in

$$\begin{aligned} \mathbf{E}(\mathbf{x}, \omega) = & \frac{(e/c)v^2 k}{(2\pi)^{1/2}} \int d\psi \int d\epsilon \exp[-ikr \cos(\epsilon - \alpha)] \cos\psi \\ & \times \exp(-ikz \sin\psi) \left[ \mathbf{k} i^\nu \sin\psi \cos\psi J_\nu(\nu \cos\psi) / \nu \cos\psi \right. \\ & \quad - \mathbf{i} \left[ \frac{i^{\nu-1}}{\nu} \cos\epsilon J'_\nu(\nu \cos\psi) + \sin\epsilon \sin^2\psi i^\nu J_\nu(\nu \cos\psi) / \nu \cos\psi \right] \\ & \quad \left. + \mathbf{j} \left[ \frac{i^{\nu-1}}{\nu} \sin\epsilon J'_\nu(\nu \cos\psi) - \cos\epsilon \sin^2\psi i^\nu J_\nu(\nu \cos\psi) / \nu \cos\psi \right] \right], \end{aligned} \quad (2.16)$$

where

$$\nu = kR = \omega T / 2\pi = \omega / \omega_0. \quad (2.17)$$

To reach (2.16) we have employed the approximation

$$J_\nu(x) = \frac{i^{-\nu}}{2\pi} \int_0^{2\pi} \exp(ix \cos\varphi - i\nu\varphi) d\varphi + O(1/\nu). \quad (2.18)$$

The  $\epsilon$  integration may be performed without approximation to yield

$$\begin{aligned} \mathbf{E}(\mathbf{x}, \omega) = & (e/c)v^2 k (2\pi)^{1/2} \int \exp(-ikz \sin\psi) \cos\psi d\psi \\ & \times \exp(-i\nu\alpha) \left[ \mathbf{k} i^{2\nu} \sin\psi \cos\psi J_\nu(\nu \cos\psi) / \nu \cos\psi J_\nu(kr \cos\psi) \right. \\ & \quad + i^\nu \sin^2\psi J_\nu(\nu \cos\psi) / \nu \cos\psi [ -(\mathbf{j} \cos\alpha + \mathbf{i} \sin\alpha) i^{\nu-1} J'_\nu(kr \cos\psi) \\ & \quad \quad \quad - (\mathbf{j} \sin\alpha - \mathbf{i} \cos\alpha) i^\nu J_\nu(kr \cos\psi) / kr \cos\psi ] \\ & \quad + \frac{i^{\nu-1}}{\nu} J'_\nu(\nu \cos\psi) [ -(\mathbf{j} \cos\alpha + \mathbf{i} \sin\alpha) i^{\nu-1} J'_\nu(kr \cos\psi) \\ & \quad \quad \quad - (\mathbf{j} \sin\alpha - \mathbf{i} \cos\alpha) i^\nu J_\nu(kr \cos\psi) / kr \cos\psi ] \left. \right]. \end{aligned} \quad (2.19)$$

As we may anticipate (2.19) to assume its familiar far-field form when  $r$  becomes large we write

$$J_\nu(kr \cos\psi) = J_\nu((vr/R)\cos\psi) \quad (2.20)$$

and, for simplicity, consider only the case for which

$$(r/R)\cos\psi > 1 \quad (2.21)$$

(which constrains, essentially, the field point  $P$ , Fig. 1, to lie outside the electron orbit). Under these circumstances the Bessel function may be replaced by its expansion of similar order and argument:<sup>13</sup>

$$\begin{aligned} J_\nu(\nu \sec\xi) \sim & \left(\frac{1}{12} \tan\xi\right)^{1/2} \{ \exp[-i\nu(\tan\xi - \frac{1}{3}\tan^3\xi - \xi) + i\pi/6] H_{1/3}^{(1)}(\frac{1}{3}\nu \tan^3\xi) \\ & + \exp[i\nu(\tan\xi - \frac{1}{3}\tan^3\xi - \xi) - i\pi/6] H_{1/3}^{(2)}(\frac{1}{3}\nu \tan^3\xi) \} \end{aligned} \quad (2.22)$$

with an error, at worst,<sup>13</sup> of  $O(\nu^{-1/2})$ . This is the most severe constraint on  $\nu$ .

When, say,

$$(\nu/3)\tan^3\xi > 10 \quad (2.23)$$

the Hankel functions may be replaced by their asymptotic expansion

$$H_{1/3}^{(2),(1)}(x) \sim \sqrt{2/(\pi x)} \exp[\pm(ix - i\pi/6 - i\pi/4)] \quad (2.24)$$

and hence

$$J_\nu(\nu \sec\xi) \sim \sqrt{6/\pi\nu \tan\xi} \cos(\nu \tan\xi - \nu\xi - \pi/4) \quad (2.25)$$

and

$$J'_\nu(\nu \sec\xi) \sim \sqrt{6/\pi\nu \tan\xi} \sin\xi \sin(\nu \tan\xi - \nu\xi - \pi/4).$$

Substituting Eqs. (2.24) and (2.25) into (2.18) and noting in addition that

$$\nu/kr \cos\psi = \cos\xi \quad (2.26)$$

we have

$$\begin{aligned} \mathbf{E}(\mathbf{x}, \omega) = & (e/c)\nu^2 k \int_{-\pi+i\infty}^{0-i\infty} (\cos\psi/\sqrt{\nu \tan\xi}) d\psi \{ \mathbf{k} i^{2\nu} \sin\psi \cos\psi J_\nu(\nu \cos\psi)/\nu \cos\psi \\ & - i^{2\nu} \sin^2\psi [J_\nu(\nu \cos\psi)/\nu \cos\psi] [\mathbf{j} \sin(\alpha - \xi) + \mathbf{i} \cos(\alpha - \xi)] \\ & + i^{2\nu-1} J'_\nu(\nu \cos\psi) [\mathbf{j} \cos(\alpha - \xi) - \mathbf{i} \sin(\alpha - \xi)] \} \\ & \times \exp\{-i[kz \sin\psi - \nu \tan\xi - \nu(\alpha - \xi) - \pi/4]\}, \end{aligned}$$

provided, from Eqs. (2.23) and (2.26),

$$(r^2 \cos^2\psi - R^2)^{3/2} > 30R^2/k. \quad (2.28)$$

The factor of 30 appearing in (2.28) is to an extent arbitrary. It follows from the asymptotic approximation of the Hankel function (2.24) and it may be argued that this is a rather conservative estimate. However, the presence of the cube in (2.28) makes a detailed discussion unnecessary. We postpone discussion of this limit to continue with the evaluation of (2.26), which is suitable for a straightforward application of the method of steepest descents. The phase  $\Psi$  of the exponential in (2.26) is stationary at some  $\psi_0$  when

$$\left. \frac{d\Psi}{d\psi} \right|_{\psi_0} = 0 \quad (2.29)$$

or

$$(r^2 \cos^2\psi_0 - R^2)^{1/2} \tan\psi_0 = z \cos\psi_0. \quad (2.30)$$

For small  $\psi_0$ , (2.29) becomes

$$\tan\psi_0 = z/(r^2 - R^2)^{1/2}. \quad (2.31)$$

The geometric significance of this equation may be seen from Fig. 2. Equation (2.30) identifies a ray connecting the field point to the orbit and lying in the tangent plane. That (2.30) only supports this interpretation when  $\psi_0$  is small is to be expected, as the importance of the tangent ray lies in the fact that it is nearly parallel to the electron velocity vector, a coincidence which is only true for field points close to the plane of the electron orbit.

To the same level of approximation the second derivative of the phase at  $\psi_0$  is

$$\left. \frac{d^2\Psi}{d\psi^2} \right|_{\psi_0} = (r^2 - R^2)^{1/2} \quad (2.32)$$

and identifying the length of the tangent ray to be

$$\kappa = (r^2 - R^2)^{1/2} / \cos\psi_0 \quad (2.33)$$

the steepest-descent integration of (2.27) yields

$$\mathbf{E}(\mathbf{x}, \omega) = (e/c)\nu(2\pi)^{1/2} \exp(-i\{k\kappa - \nu[\alpha - \xi(\psi_0)]\}) \times \left[ \mathbf{k} i^{2\nu} \sin\psi_0 \cos\psi_0 J_\nu(\nu \cos\psi_0) / \nu \cos\psi_0 - i^{2\nu} \sin^2\psi_0 [J_\nu(\nu \cos\psi_0) / \nu \cos\psi_0] \{ \mathbf{j} \sin[\alpha - \xi(\psi_0)] + \mathbf{i} \cos[\alpha - \xi(\psi_0)] \} + \frac{i^{2\nu-1}}{\nu} J'_\nu(\nu \cos\psi_0) \{ \mathbf{j} \cos[\alpha - \xi(\psi_0)] - \mathbf{i} \sin[\alpha - \xi(\psi_0)] \} \right] \quad (2.34)$$

subject to the restriction that the field of  $O(1/\nu^{1/2})$  may be neglected,  $\psi_0$  is small and (2.28) satisfied.

In the far field of the synchrotron radiation it is more convenient to work with coordinates specific to the tangent ray. From Fig. 2 the angle  $\alpha - \xi(\psi_0)$  can be identified as the angle between the  $x$  axis and the projection of the tangent ray onto the plane of the electron orbit. Writing this angle as  $\beta$  and introducing the vectors

$$\epsilon_{||} = \mathbf{j} \sin\beta + \mathbf{i} \cos\beta, \quad \epsilon_{\perp} = \mathbf{j} \cos\beta - \mathbf{i} \sin\beta, \quad (2.35)$$

so that  $\epsilon_{\perp}$  is the unit vector in the plane of the orbit transverse to the tangent ray, (2.34) may be written

$$\mathbf{E}(\kappa, \psi_0, \nu) = (2\pi)^{1/2} \nu (e/c) \exp[-i(k\kappa + \nu\beta)] [i^{2\nu} (\mathbf{k} \sin\psi_0 \cos\psi_0 - \epsilon_{||} \sin^2\psi_0) J_\nu(\nu \cos\psi_0) / \cos\psi_0 + i^{2\nu-1} \epsilon_{\perp} J'_\nu(\nu \cos\psi_0)] \quad (2.36)$$

which identifies the field in the plane of the orbit to be transversely polarized.

It is convenient at this point to recall the important features of this result. The power radiated into unit angular frequency interval and unit solid angle is given by

$$P(\psi_0, \nu) d\psi_0 d\omega = \frac{c^2}{8\pi^2 R} \kappa^2 [ |\mathbf{E}(\psi_0, \nu)|^2 + |\mathbf{E}(\psi_0, -\nu)|^2 ] \quad (2.37)$$

and substituting Eq. (2.36) into Eq. (2.37) we find

$$P(\psi_0, \nu) d\psi_0 d\omega = \frac{(e\nu)^2}{2\pi R} \{ [J'_\nu(\nu \cos\psi_0)]^2 + \sin^2\psi_0 [J_\nu(\nu \cos\psi_0) / \cos\psi_0]^2 \} \quad (2.38)$$

which is Schwinger's result.<sup>6</sup>

The radiated power spectrum of (2.38) can be put in its more familiar form by following Schwinger and replacing the Bessel functions with their asymptotic representation for large argument and larger order [as distinct from large order and larger argument, (2.22)] to find

$$P(\psi_0, \nu) d\psi_0 d\omega = \frac{(\psi_0^2 e\nu)^2}{6\pi^3 R} \{ [K_{2/3}(\nu\psi^3/3)]^2 + [K_{1/3}(\nu\psi^3/3)]^2 \} \quad (2.39)$$

which describes a power spectrum which is concentrated to a small range of angles  $\psi_0$  about 0. When  $\psi_0=0$ , the spectrum takes its maximum value of

$$P(0, \nu) d\psi_0 d\omega = \frac{e^2}{2\pi^3 R} \left[ \frac{3}{4} \right]^{1/3} \Gamma^2\left(\frac{2}{3}\right) \nu^{2/3}. \quad (2.40)$$

The modified Bessel functions decay rapidly away to zero when their argument exceeds 1, which, after Jackson,<sup>12</sup> we take to define the angular width of the spectrum at low frequencies:

$$\psi_w = (3/\nu)^{1/3}. \quad (2.41)$$

Associated with this angle is a length of track

$$L_w = R\psi_w. \quad (2.42)$$

This length is a measure of the length of electron orbit which contributes to the radiated field at a particular point.

The significance of the limit (2.28) is that it defines a distance  $\kappa_0$  from the tangent point

$$\kappa_0 = 2L_w, \quad (2.43)$$

beyond which the field assumes its  $1/\kappa$  dependence. Only at ranges greater than  $\kappa_0$  does the field assume its spherical spreading form. Thus, for an aperture placed at some distance  $\kappa < \kappa_0$ , brightness and total power estimates,

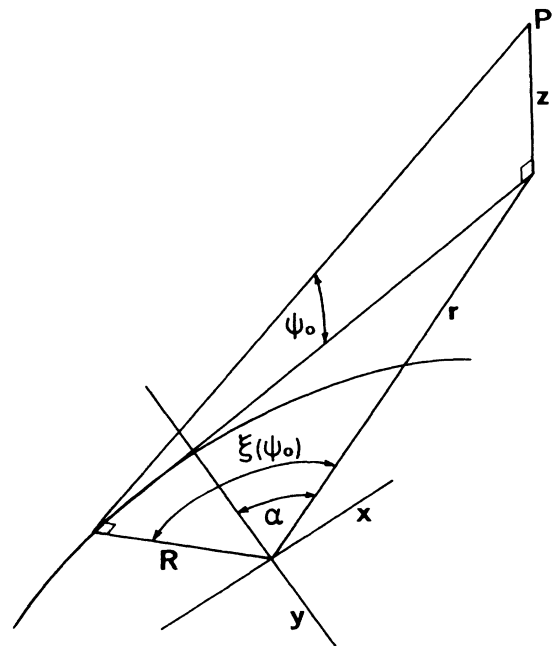


FIG. 2. The geometry of the tangent ray between the electron orbit and the field point  $P$ . The ray is so defined that its projection onto the  $x$ - $y$  plane forms a tangent to the electron orbit.

based on Eq. (2.39), will be significant overestimates, in rough proportion to  $\kappa_0^2 \cdot \kappa^2$ .

It is desirable to have a simple explanation of this result. We might anticipate that  $\kappa_0$  is simply related to the distance at which the arc length  $R\psi_w$  subtends the first Fresnel zone at the point  $P$  in Fig. 2. This is indeed the case. The highest-order term in  $\psi_w$  neglected in the far-field phase approximation is  $R^2\psi_w^4/2\kappa$ . The arc length  $R\psi_w$  will subtend the first Fresnel zone when this term equals  $\lambda/4$ . This will occur at a distance  $\kappa_{fz} = kR^2\psi_w^4/\pi = R\psi_w = \kappa_0/\pi$ .

### III. THE EFFECT OF A FINITE CURVED TRACK LENGTH

In many synchrotrons the track followed by the electrons is not a circle, but a number of circular arcs connected by linear sections. The arc lengths are typically very much smaller than the  $2\pi R$  assumed in the source distribution of (2.4)–(2.7). However, at high frequencies

the length of electron orbit,  $L_w$ , contributing to the radiated field at a particular point is very small indeed and it is safe to ignore any effects caused by the truncation of the source distribution at the edges of the arcs.

In the far infrared this is no longer true, and  $L_w$  may approach the arc length of the electron track.<sup>10</sup> In this section we describe the effect that the truncation of the source distribution has on the radiated field, restricting the discussion to the far field of the synchrotron radiation.

The finite arc length may be introduced by replacing (2.7) with

$$-R\phi_t/c \leq t \leq R\phi_t/c \quad (3.1)$$

so that the circular arc subtends an angle of  $2\phi_t$  in the plane of the orbit. In the far field of the synchrotron, it is neither necessary to distinguish between the angles  $\alpha$  and  $\beta$ , nor distinguish a particular value of  $\psi$  by  $\psi_0$ , so that we may set

$$\frac{\exp(-ik|\mathbf{x}-\mathbf{R}|)}{|\mathbf{x}-\mathbf{R}|} \sim \frac{\exp\{-ik[|\mathbf{x}-\mathbf{R}\mathbf{j}| + \mathbf{R}\cdot(\mathbf{x}-\mathbf{R}\mathbf{j})/|\mathbf{x}-\mathbf{R}\mathbf{j}|]\}}{|\mathbf{x}-\mathbf{R}\mathbf{j}|} \quad (3.2)$$

in (2.9) and (2.10). From (2.11), (2.31), (2.33), and (2.35), we find

$$\mathbf{E}(\kappa, \psi, \beta, \nu) = \frac{-\nu\phi_t \exp(-ik\kappa)}{\omega_0\kappa\sqrt{2\pi}} \int_{-1-\beta/\phi_t}^{1-\beta/\phi_t} \{\epsilon_{\perp} \sin(\phi_t\tau) - \epsilon_{\parallel} [\cos\psi - \cos(\phi_t\tau)] + \mathbf{k} \sin\psi\} \exp\{-i[\nu\phi_t\tau + \nu \sin(\phi_t\tau)]\} \, d\tau \quad (3.3)$$

where we note that the introduction of noncircular symmetry results in the field being a function of both  $\psi$  and  $\beta$ . From (2.37) and (2.39) we may define a power gain

$$G(\psi, \beta, \nu, \phi_t) = \frac{P(\psi, \beta, \nu, \phi_t)}{P(\psi, \nu)} \quad (3.4)$$

to be the ratio of the power radiated per unit solid angle in the direction  $\psi, \beta$  to the power radiated in the absence of any truncation.

At sufficiently high frequencies (3.3) may be approximated asymptotically. Provided  $|\beta| < \phi_t$ ,

$$G(\psi, \beta, \nu) \sim 1 \quad (3.5)$$

(see, for example, Jackson<sup>12</sup>). If  $|\beta| > \phi_t$ , the phase in (3.4) is nowhere stationary between  $+\phi_t$  and  $-\phi_t$ , and it can be shown that

$$G(\psi, \beta, \nu) \sim \nu^{-1} \quad (3.6)$$

Equations (3.5) and (3.6) provide the geometric optical description of the effect of the source truncation. When  $|\beta| < \phi_t$  the point  $P$  lies in a region of constant illumination. When  $|\beta|$  exceeds  $\phi_t$ ,  $P$  lies in the geometric shadow.

At lower frequencies there does not appear to be any simple asymptotic solution to (3.3), and we are thus led to investigate (3.3) numerically. As it stands (3.3) will not nondimensionalize further. However, for values of  $\phi_t \ll 2\pi$ ,  $G(\psi, \beta, \nu, \phi_w)$  is, to a good approximation, a function of  $\psi, \beta/\phi_t$  and  $\nu^{1/3}\phi_t = 3^{1/3}\phi_t/\psi_t \equiv \mu$  only; as may be seen by expanding the exponential in the integrand

of (3.3). To confirm this conclusion, and investigate the behavior of  $G(\psi, \beta/\phi_t, \mu)$ , (3.3) has been numerically integrated. A simple Simpson's rule scheme was implemented. The number of points in the interval was determined by requiring that there be at least 20 points per wavelength at the highest frequency of oscillation on the interval  $-1-\beta/\phi_t, 1-\beta/\phi_t$ . To check the scheme, the program was used to compute  $P(0, \nu)$  [Eq. 2.40], for values of  $\nu < 10000$ , and found to be in error by  $< 0.1\%$ .

Figure 3(a) shows the function  $G_1 = G(0, 0, \mu, \phi_t = 0.025)$ . Figures 3(b), 3(c), 3(d), and 3(e) show the ratio  $G(0, 0, \mu, \phi_t)/G_1$  for values of  $\phi_t = 0.05, 0.1, 0.2$ , and  $0.4$ , respectively. In keeping with the remarks above,  $G(0, 0, \mu, \phi_t)$  can be seen to have only a very weak dependence on  $\phi_t$ . This result demonstrates that the crucial factor in determining the field in the presence of a truncated source is the number of wavelengths, given by  $\mu/\pi$ , radiated by the electron in passing from  $-\phi_t$  to  $\phi_t$ .

Figure 3(a) may be explained in these terms. When  $\mu \ll \pi$  contributions from across the entire arc are in phase and  $G(0, 0, \phi)$  varies as  $\phi_t^2$ . When  $\mu \gg \pi$ , the effects of the edges of the arc become negligible and (3.5) holds. When  $\mu \sim \pi$  the edges play an important role in determining the radiated power distribution. The oscillations seen in Fig. 3(a) may be interpreted as interference between contributions from either end of the arc.

Figures 4, 5, and 6 show the gain  $G(0, \beta/\phi_t, \mu)$  for  $\mu = 1.5, 3$ , and  $10$ , respectively. The same behavior is seen in this figure. At small values of  $\mu$ , the field in the orbit of the electrons is dominated by diffraction from the edges of the arc. Considerable energy has been radiated

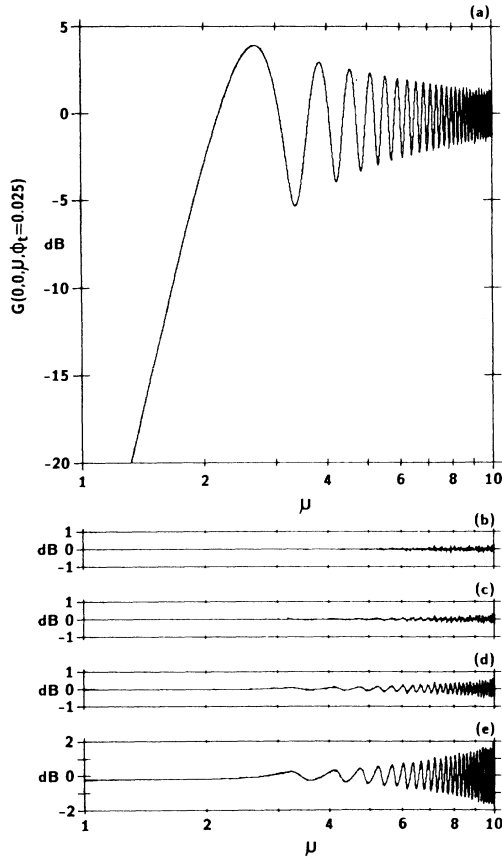


FIG. 3. (a) The power gain  $G(0,0,\mu,\phi_t)$  in the synchrotron spectrum, on the axis of the synchrotron beam, when the circular section of the electron orbit subtends an angle  $2\phi_t$ , over that power radiated with a truly circular orbit. (b)  $G_1 = G(0,0,\mu,\phi_t=0.025)$ ; (c)  $G(0,0,\mu,\phi_t=0.1)/G_1$ ; (d)  $G(0,0,\mu,\phi_t=0.2)/G_1$ ; (e)  $G(0,0,\mu,\phi_t=0.4)/G_1$ .

into the shadow region of (3.6), with a consequent loss when  $\beta/\phi_t=0$  of 15 dB. As  $\mu$  increases, the diffraction effects reduce, although their effect is still marked at  $\mu=3$ . By the time  $\mu=10$ , however, the fields tends to that described by (3.5) and (3.6), i.e., a region of constant illumination bounded by a shadow.

#### IV. THE STATISTICS OF THE RADIATED FIELD

Thus far, we have considered only the field radiated from a single electron. The field radiated by the electron synchrotron is the sum of the fields radiated by successive bunches of  $\sim 10^{10}$  electrons. In this section we consider the consequences of the electron bunch, and successive bunches, on the radiated field.

The total field radiated by a succession of electron bunches is

$$\mathbf{E}_T(\mathbf{x},\omega) = \sum_{j=-K}^K \mathbf{E}_B(\mathbf{x},\omega)_j \exp(-i\omega t_j), \quad (4.1)$$

where  $t_j$  is the time at which the center of the bunch passes the tangent point from the orbit to the point  $x$ , and

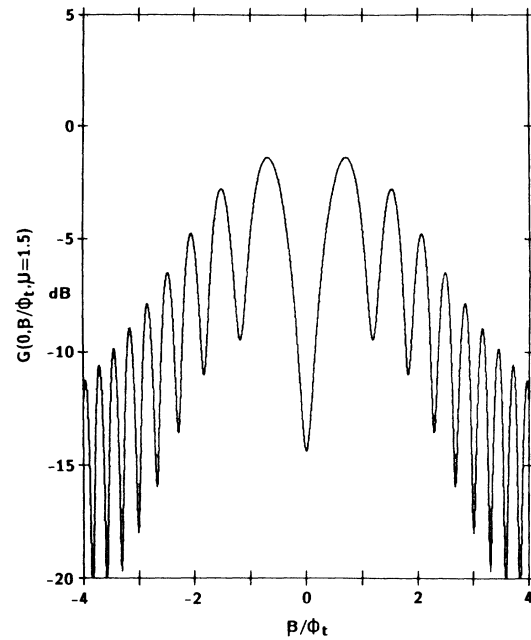


FIG. 4. The power gain  $G(0,\beta/\phi_t,\mu=1.5)$  in the synchrotron spectrum, in the plane of the electron orbit, when the circular section of the electron orbit subtends an angle  $2\phi_t$ , over that power radiated with a truly circular orbit.

$\mathbf{E}_B(\mathbf{x},\omega)$  is the field radiated by a single bunch of  $N$  electrons:

$$\mathbf{E}_B(\mathbf{x},\omega) = \sum_{i=1}^N \mathbf{E}(\mathbf{x},\omega)_i \exp(-i\omega t_i) \quad (4.2)$$

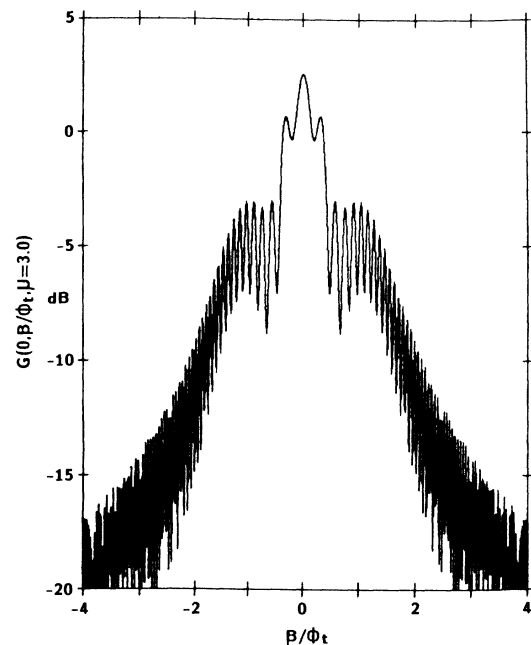


FIG. 5. The power gain  $G(0,\beta/\phi_t,\mu=3)$  in the synchrotron spectrum, on the plane of the electron orbit, when the circular section of the electron orbit subtends an angle  $2\phi_t$ , over that power radiated with a truly circular orbit.

and  $t_i$  is the time at which a particular electron passes the same tangent point on the orbit. We define the functions

$$\mathbf{A}(\mathbf{x}_1, \mathbf{x}_2, \omega) = (c/2\pi) \langle \mathbf{E}(\mathbf{x}_1, \omega) \cdot \mathbf{E}^*(\mathbf{x}_2, \omega) \rangle \quad (4.3)$$

and

$$C(\mathbf{x}_1, \mathbf{x}_2, \omega) = \frac{|\mathbf{A}(\mathbf{x}_1, \mathbf{x}_2, \omega)|}{[|\mathbf{A}(\mathbf{x}_1, \mathbf{x}_1, \omega)| |\mathbf{A}(\mathbf{x}_2, \mathbf{x}_2, \omega)|]^{1/2}} \quad (4.4)$$

so that, for  $\mathbf{x}_1 = \mathbf{x}_2$ ,  $\mathbf{A}(\mathbf{x}_1, \omega)$  is the mean radiated energy per unit solid angle, and  $C(\mathbf{x}_1, \mathbf{x}_2, \omega)$  is the spatial correlation coefficient between the fields at  $\mathbf{x}_1$  and  $\mathbf{x}_2$ .

In the calculation of these functions a considerable simplification arises if the assumption is made that the position of each electron is a random variable which is independent of any other electron position, i.e.,

$$\langle \mathbf{R}(t)_{ij} \cdot \mathbf{R}(t)_{mk} \rangle = \langle \mathbf{R}(t)_{ij} \rangle \cdot \langle \mathbf{R}(t)_{mk} \rangle, \quad i \neq m, \quad j \neq k. \quad (4.5)$$

I have been unable to find a demonstration of this result in the literature, although its use is fairly universal. It is not our purpose here to examine this difficult area. We will assume (4.5) is true, and merely note that we know of no evidence to suggest otherwise.

With this assumption (4.3) becomes

$$\begin{aligned} \mathbf{A}(\mathbf{x}_1, \mathbf{x}_2, \omega) = & (c/2\pi) \left\langle \sum_j \mathbf{E}_B(\mathbf{x}_1, \omega)_j \exp(-i\omega t_j) \right\rangle \cdot \left\langle \sum_k \mathbf{E}_B^*(\mathbf{x}_2, \omega)_k \exp(-i\omega t_k) \right\rangle \\ & + (c/2\pi) \left\langle \sum_j \mathbf{E}(\mathbf{x}_1, \omega)_{Bj} \cdot \mathbf{E}(\mathbf{x}_2, \omega)_{Bj}^* \right\rangle, \quad j \neq k. \end{aligned} \quad (4.6)$$

Equation (4.6) requires us to find the mean and mean-square fields from a single electron bunch:  $\langle \mathbf{E}_B(\mathbf{x}_1, \omega) \rangle$  and  $\langle \mathbf{E}_B(\mathbf{x}_1, \omega) \cdot \mathbf{E}_B^*(\mathbf{x}_2, \omega) \rangle$ , respectively. The mean field is

$$\langle \mathbf{E}_B(\mathbf{x}_1, \omega)_j \rangle = \sum_i \mathbf{F}_{ij}(\kappa, \psi, \nu) \exp[-i(k\kappa_{ij} + \nu\beta_{ij} + \omega t_{ij})], \quad (4.7)$$

where we have employed (2.36) and (4.2) and set

$$\mathbf{F}(\kappa, \psi, \nu) = (2\pi)^{1/2} \nu (e/c) [i^{2\nu} (\mathbf{k} \sin\psi_0 \cos\psi_0 - \epsilon_{\parallel} \sin^2\psi_0) J_{\nu}(\nu \cos\psi_0) / \cos\psi_0 + i^{2\nu-1} \epsilon_{\perp} J'_{\nu}(\nu \cos\psi_0)]. \quad (4.8)$$

We now assume that the electron bunches are distributed uniformly around the orbit so that they pass a particular point at intervals of time  $\tau_B$ . For convenience we define the time origin to be the time at which the center of the zeroth bunch passes the tangent point from the orbit to  $\mathbf{x}_1$  so that

$$t_j = j\tau_B. \quad (4.9)$$

The bunches are assumed to be statistically identical so that  $\langle \diamond_{ij} \rangle = \langle \diamond_i \rangle$ . Each one is distributed around a central electron whose orbit radius is  $R$  and which lies in the plane  $z=0$ . The  $i$ th electron is assumed to have an orbit radius  $R+\eta$ , lie in the plane  $z=\zeta$ , and pass the origin at a time  $t_1$  later than the central electron. The values of  $\kappa$ ,  $\beta$ , and  $\psi$  in the phase of the exponential in (4.7) are functions of the electron orbit radius  $R+\eta$  and height  $\zeta$  through (2.31). Expanding this phase to second order in

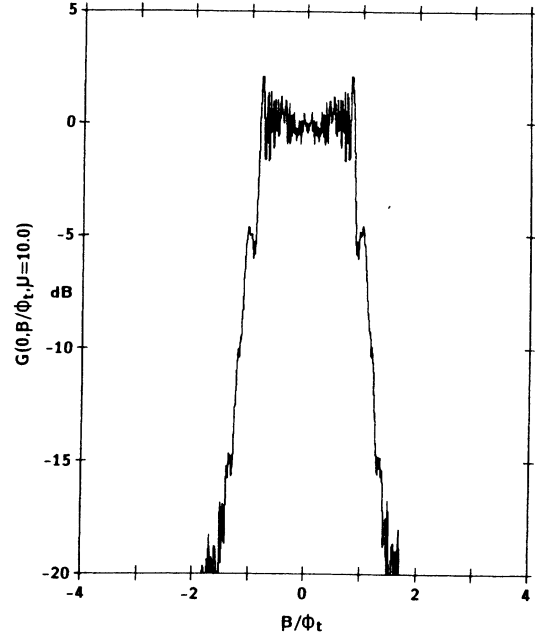


FIG. 6. The power gain  $G(0, \beta/\phi_t, \mu=10.0)$  in the synchrotron spectrum, on the plane of the electron orbit, when the circular section of the electron orbit subtends an angle  $2\phi_t$ , over that power radiated with a truly circular orbit.

the quantities  $\eta$  and  $\zeta$  we find

$$\begin{aligned} k\kappa_1 + \nu\beta_i \sim & k[\kappa + R\beta - \psi\zeta_i + \beta\eta_i - (3/2\kappa)\eta_i^2 \\ & + (1/2\kappa)\zeta_i^2], \end{aligned} \quad (4.10)$$

where the values  $\kappa$ ,  $\beta$ , and  $\psi$  refer to the tangent ray from the central electron. For a high brightness machine such as the Daresbury (post HBL) synchrotron radiation spectrum (SRS),  $\eta$  is typically  $\sim 10^{-3}$  m and  $\zeta \sim 0.15 \times 10^{-3}$  m. Assuming  $\psi < 0.1$  to satisfy (2.31) and  $\kappa > 1.0$  m to satisfy (2.28), only the linear terms in (4.10) need be retained. In addition, a close examination of (2.22) and (2.23) shows that satisfying (2.28) ensures that  $F$  is slowly varying in comparison with the exponential in (4.7). Thus, for the frequencies of interest,

$$\langle \mathbf{E}_B(\mathbf{x}, \omega) \rangle = N \mathbf{E}(\mathbf{x}, \omega) \langle \exp(-i\omega\tau_i) \rangle, \quad (4.11) \quad \langle \mathbf{E}_B(\mathbf{x}_1, \omega) \cdot \mathbf{E}_B^*(\mathbf{x}_2, \omega) \rangle = \langle \mathbf{E}_B(\mathbf{x}_1, \omega) \rangle \cdot \langle \mathbf{E}_B^*(\mathbf{x}_2, \omega) \rangle$$

where we have set

$$\tau_i = (\beta\eta_i - \psi\xi_i)/c + t_i. \quad (4.12)$$

The second term we require is the mean-squared field from a single bunch:

$$\langle \mathbf{E}_B(\mathbf{x}_1, \omega) \cdot \mathbf{E}_B^*(\mathbf{x}_2, \omega) \rangle = \mathbf{E}(\mathbf{x}_1, \omega) \cdot \mathbf{E}^*(\mathbf{x}_2, \omega)$$

$$\times (N^2 \langle \exp[-i\omega\tau(\mathbf{x}_1)_i] \rangle \langle \exp[i\omega\tau(\mathbf{x}_2)_i] \rangle + N \langle \exp\{-i\omega[\tau_i(\mathbf{x}_1) - \tau_i(\mathbf{x}_2)]\} \rangle). \quad (4.14)$$

We remark at this point that the results of both Bernard and Rousseau<sup>10</sup> and Akhmanov<sup>11</sup> may be deduced from this formula, in spite of the latter's claim to contradict the former. Assuming that  $\psi(\mathbf{x}_1) = \psi(\mathbf{x}_2) = 0$ , that the quantities  $t_i$ ,  $\eta_i$ , and  $\xi_i$  are Gaussian distributed (as we shall presently), and that  $\tau(\mathbf{x}_1) \sim \tau(\mathbf{x}_2)$  in the coherent term in  $N^2$ , (4.14) becomes Eq. (44) of Ref. 10. Alternatively, if the frequency is assumed sufficiently high that the coherent term is negligible and (4.12) is substituted into (4.14) we reach Eq. (2.6) of Ref. 11 on allowing for the differing coordinate choice.

Equations (4.11) and (4.14) may be used to provide a general expression for the spatial and temporal coherence of the synchrotron radiation. It is, however, more instructive to give the characteristic functions a particular form which we take to be Gaussian; that is, we assume the joint probability density function of  $t_i$ ,  $\eta_i$ , and  $\xi_i$  to be

$$p(t_i < t, \eta_i < \eta, \xi_i < \xi) dt d\eta d\xi = \frac{(2\pi)^{-3/2}}{\sigma_t \sigma_\eta \sigma_\xi} \exp[-(t^2/\sigma_t^2 + \eta^2/\sigma_\eta^2 + \xi^2/\sigma_\xi^2)/2] dt d\eta d\xi \quad (4.15)$$

in keeping with (4.5).

From (4.3), (4.9), (4.11), (4.14), and (4.15) the mean radiated energy per unit solid angle is

$$\mathbf{A}(\mathbf{x}, \omega) = (c/2\pi) \mathbf{E}(\mathbf{x}, \omega) \cdot \mathbf{E}^*(\mathbf{x}, \omega) \left[ N^2 \frac{\sin^2[\omega(K + \frac{1}{2})\tau_B]}{\sin^2(\omega\tau_B/2)} \exp[-2k^2(\sigma_t^2 c^2 + \psi^2 \sigma_\xi^2 + \beta^2 \sigma_\eta^2) + N(2K + 1)] \right] \quad (4.16)$$

which may be converted to power by multiplying by  $1/(2K + 1)\tau_B$ .

The energy spectrum of (4.16) contains two terms, which may be identified as the coherent component, proportional to  $N^2$ , and the incoherent component, proportional to  $N$ . The coherent component is, more or less, a line spectrum, resulting from the interference between the separate bunches. Each line has a maximum when

$$\omega = n\omega_B, \quad n = \dots, -1, 0, 1, \dots, \quad (4.17)$$

where

$$\omega_B = 2\pi/\tau_B, \quad (4.18)$$

taking a value of the maximum of

$$(c/2\pi) N^2 |\mathbf{E}(\mathbf{x}, n\omega_B)|^2 (2K + 1)^2 \exp[-2(n\omega_B/c)^2 (\sigma_t^2 c^2 + \psi^2 \sigma_\xi^2 + \beta^2 \sigma_\eta^2)] \quad (4.19)$$

and whose width is

$$\Delta\omega = \omega/(2K + 1). \quad (4.20)$$

When  $\beta = \psi = 0$ , the coherent and incoherent components are equal in amplitude when

$$\omega = \omega_c = \sigma_t^{-1} \{\ln[N(2K + 1)]\}^{1/2}. \quad (4.21)$$

From (4.21) it is apparent that the crossover point between the coherent and incoherent is a function of the number of bunches. In any measurement this will be determined by the resolution of the measuring instrument (and not the integration time of the experiment).

The spatial coherence between the points  $\mathbf{x}_1$  and  $\mathbf{x}_2$  is

$$C(\mathbf{x}_1, \mathbf{x}_2, \omega) = \frac{\mathbf{E}(\mathbf{x}_1, \omega) \cdot \mathbf{E}^*(\mathbf{x}_2, \omega)}{[\mathbf{A}(\mathbf{x}_1, \omega) \mathbf{A}(\mathbf{x}_2, \omega)]^{1/2}} \times \left[ N^2 \frac{\sin^2[\omega(K + 1/2)\tau_B]}{\sin^2(\omega\tau_B/2)} \exp(-k^2 \{ 2\sigma_t^2/c^2 + \sigma_\eta^2 [\beta^2(x_1) + \beta^2(x_2)] + \sigma_\xi^2 [\psi^2(x_1) + \psi^2(x_2)] \}) + N(2K + 1) \exp(-k^2 \{ \sigma_\eta^2 [\beta(x_1) - \beta(x_2)]^2 + \sigma_\xi^2 [\psi(x_1) - \psi(x_2)]^2 \}) \right]. \quad (4.22)$$

The behavior of this function depends upon the relative power in the coherent and incoherent parts of the spectrum. When  $\omega \ll \omega_c$ , the field is completely coherent except when  $\mathbf{E}(\mathbf{x}_1, \omega) \cdot \mathbf{E}(\mathbf{x}_2, \omega) = 0$ .

When  $\omega \gg \omega_c$ , the coherent part of the spectrum is negligible. When  $\psi(x_1) = \psi(x_2) = 0$ , the spatial coherence is determined entirely by the angle  $\beta(x_1) - \beta(x_2)$  through which the tangent ray turns in going from  $x_1$  to  $x_2$ . This dependence may be characterized by a coherence angle  $\beta_c$ , through which the coherence drops by  $1/e$ :

$$\beta_c = (1/k\sigma_\eta)[\ln(4)]^{1/2}. \quad (4.23)$$

In a similar fashion the variation in coherence out of the plane of the orbit may be characterized by a coherence angle  $\psi_c$ :

$$\psi_c = (1/k\sigma_\zeta)[\ln(4)]^{1/2}. \quad (4.24)$$

In the far field the angular extent of an aperture in the plane of the orbit is equal to the range of angles in  $\beta$  that it subtends. Equations (4.23) and (4.24) are thus a direct measure of the spatial coherence of the synchrotron radiation across an aperture.

#### V. APPLICATION OF THE RESULTS TO HIGH-BRIGHTNESS SYNCHROTRONS

This study was started in response to concern that departures from the high-frequency form of the synchrotron spectrum in the mm region might result in lower values of flux and brightness than would otherwise be expected. In this section we examine this question by applying the results of the previous three sections to the post HBL Daresbury SRS.

In Table I the values of the lattice and beam constants<sup>13</sup> are shown, together with the values of the various parameters identified in the previous sections as characterizing the radiated power. Three sets of values are given, corresponding to the wavelengths 10, 1, and  $10^{-1}$  mm.

The first two parameters,  $\nu$  and  $\psi_w$ , are within the limits set by (2.22) and (2.31) and need no further comment. However, the near-field distances  $\kappa_0$  are surprisingly large. In a practical synchrotron, the choice of geometry is re-

stricted, and for this reason the first aperture encountered by the beam is a mirror whose task is to deflect the beam away from the orbit. Table I demonstrates that there is little to be gained from siting this mirror at distances closer than 0.5 m (say) to the tangent point. Within this range the effective length of orbit contributing to the field at the mirror is reduced by the Fresnel term in the phase of each contributing element.

The values of  $\mu$  shown in Table I show that no overall loss of power is likely to accrue from the finite length of the arc sections. However, at wavelengths greater than  $10^{-1}$  mm, the field will show considerable structure on the  $\pm 5$ -dB level. The parameter  $\mu$  is linear with  $\phi_t$ , and it can be seen from Fig. 3 that the effect of finite arc length at the low frequencies is highly dependent on the particular synchrotron geometry. For wavelengths less than  $10^{-1}$  mm, the effect of the finite arc length may be ignored for most purposes.

The values of  $\omega/\omega_c$  indicate that, at Daresbury, coherent radiation is probably negligible at these wavelengths. The value of  $K$  is determined by the resolving power of the instrument used to measure the spectrum. At mm wavelengths, resolving powers of 100 kHz are possible with heterodyne spectrometers; however, it may be seen from (4.20) that the dependence of  $\omega_c$  on  $K$  is extremely weak, and the crossover between the coherent and incoherent components of the spectrum is largely determined by the number of electrons in a bunch. It is also worth pointing out that the crossover occurs at a frequency some six times higher than the half-width of the coherent component  $\sigma_t^{-1}$ . Given this fact, it would perhaps be best not to take the Gaussian form of the coherent component at these frequencies too seriously.

The importance of the angle  $\beta_c$ , which measures the spatial coherence in the plane of the orbit, depends on the dimensions of the aperture. To give a specific example, the field over a mirror subtending 50 mrad would vary from complete spatial coherence at 10-mm wavelengths, to almost complete incoherence at  $10^{-1}$  mm. Clearly, for any particular application  $\beta_c$  is an important parameter.

Out of the plane of orbit a slightly different mechanism operates. At a 10-mm wavelength, the coherence angle  $\psi_c$

TABLE I. The parameters describing the beam, lattice, and radiated spectrum of the Daresbury (post high brightness lattice) SRS.

BEAM AND LATTICE PARAMETERS							
RADIUS	ELECTRONS PER BUNCH	NUMBER OF BUNCHES (1 MHz RESOLUTION)	BUNCH LENGTH	RADIAL BUNCH WIDTH	VERTICAL BUNCH WIDTH		
R (m)	N	K	$\sigma_t$ (sec)	$\sigma_\eta$ (m)	$\sigma_\zeta$ (m)		
5.5	$10^{10}$	$10^3$	$2 \times 10^{-10}$	$10^{-3}$	$5 \times 10^{-4}$		
RADIATED SPECTRUM PARAMETERS							
$\lambda$ (m)	$\nu$	$\kappa_0$ (m)	$\psi_w$ (rad)	$\mu$ (rad)	$\omega/\omega_c$	$\beta_c$ (rad)	$\psi_c$ (rad)
$10^{-2}$	$3 \times 10^3$	1.1	$10^{-1}$	2.9	7	$6 \times 10^{-1}$	$3 \times 10^{-1}$
$10^{-3}$	$3 \times 10^4$	0.5	$4 \times 10^{-2}$	6.5	$7 \times 10^1$	$6 \times 10^{-2}$	$3 \times 10^{-2}$
$10^{-4}$	$3 \times 10^5$	0.2	$2 \times 10^{-2}$	14.4	$7 \times 10^2$	$6 \times 10^{-3}$	$3 \times 10^{-3}$

is larger than the width of the beam, and the field may be regarded as coherent irrespective of the width of the mirror. For wavelengths less than  $10^{-1}$  mm this is no longer the case for here the coherence angle is very much less than the beam half-width.

#### ACKNOWLEDGMENTS

It is with pleasure that I record my thanks to Professor D. H. Martin of the Department of Physics, Queen Mary

College, London, for many useful discussions on the subject matter of this paper. I am grateful to Dr. Ian Munroe and members of his staff for their help and for providing the data on the post HBL Daresbury lattice. I would also like to thank Dr. Nigel Cronin, of the School of Physics, University of Bath, for introducing me to the problem, and for his advice on mm-wave instrumentation. This work was in part funded by the United Kingdom Science and Engineering Research Council.

- 
- \*Present address: Department of Electrical and Electronic Engineering, University College London, Torrington Place, London, WC1E 7JE England.
- <sup>1</sup>Daresbury Synchrotron Radiation Source (SRS), Science and Engineering Research Council, Daresbury Laboratory, Warrington WA4 4AD, UK; National Synchrotron Light Source (NSLS), Brookhaven National Laboratory, Upton, New York, 11973; Berliner Elektronenspeicherring-Gesellschaft f. Synchrotronstrahlung MbH BESSY, D-1000 Berlin, 33, West Germany.
- <sup>2</sup>J. R. Stevenson, H. Ellis, and R. Bartlett, *Appl. Opt.* **12**, 2884 (1983).
- <sup>3</sup>J. R. Stevenson and J. M. Cathcart, *Nucl. Instrum. Methods* **172**, 367 (1980).

- <sup>4</sup>P. Lagarde, *Infrared Phys.* **18**, 395 (1978).
- <sup>5</sup>W. D. Duncan and G. P. Williams, *Appl. Opt.* **22**, 2914 (1983).
- <sup>6</sup>J. Schwinger, *Phys. Rev.* **75**, 1912 (1949).
- <sup>7</sup>N. M. Blachman and E. D. Courant, *Rev. Sci. Instrum.* **20**, 596 (1949).
- <sup>8</sup>F. C. Michel, *Phys. Rev. Lett.* **48**, 580 (1982).
- <sup>9</sup>M. Sands, *Phys. Rev.* **97**, 470 (1955).
- <sup>10</sup>C. Benard and M. Rousseau, *J. Opt. Soc. Am.* **64**, 1433 (1974).
- <sup>11</sup>S. A. Akhmanov, B. A. Grishanin, G. A. Lyakov, and Y. V. Ponomarev, *Fizika* **35**, 31 (1980).
- <sup>12</sup>J. D. Jackson, *Classical Electrodynamics*, 3rd ed. (Wiley, New York, 1963).
- <sup>13</sup>G. N. Watson, *Proc. Cambridge Philos. Soc.* **19**, 96 (1918).